Soft Matter

Dynamic Article Links

Cite this: *Soft Matter*, 2012, **8**, 10549

www.rsc.org/softmatter

REVIEW

Exploring emulsion science with microfluidics

Nicolas Bremond* and Jérôme Bibette

Received 20th April 2012, Accepted 31st May 2012
DOI: 10.1039/c2sm25923k

Emulsions have been studied for a long time because of the richness of their related fundamental physicochemical phenomena and owing to their wide industrial applications. The development of microfluidics offers new opportunities to investigate emulsion features and behaviours. This review relates the use of microfluidic tools for probing the interfacial properties of emulsion droplets and the two main mechanisms of destabilisation, namely the coalescence of adjacent drops and the molecular transfer between neighbouring drops.

I. Introduction

Emulsions are metastable dispersions of liquid droplets into a second liquid phase with the presence of surface active agents (Fig. 1). They have been the subject of considerable fundamental and applied investigations.[1,2] One reason for this appeal is the occurrence of a rich variety of physicochemical phenomenon that mainly involve liquid interfaces. Among others, this includes coalescence, ripening, adhesion or coacervation of emulsion droplets.[3–5] In addition, some aspects of their phenomenology, for example the phase inversion of concentrated emulsions under shear, have remained poorly understood or not explored, mainly because they are difficult to access in bulk experiments. A second reason for this interest is the wide use of emulsions in industry from polymerisation, paint and road making applications, to cosmetics or food industries.

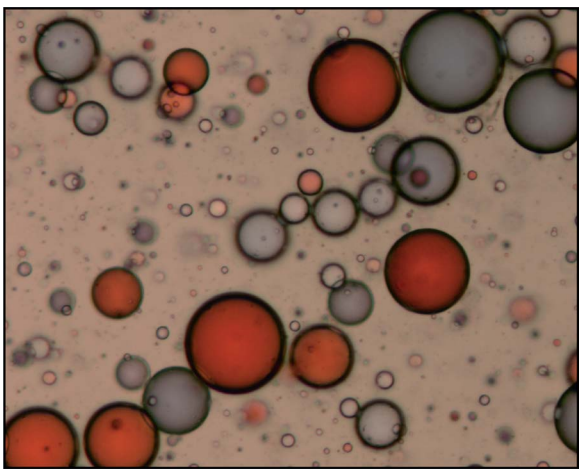

Fig. 1 Binary water-in-oil emulsion obtained by an inhomogeneous shearing.

UPMC Univ. Paris 06, CNRS UMR 7195, ESPCI ParisTech, 10 rue Vauquelin, 75231 Paris, France. E-mail: Nicolas.Bremond@espci.fr

Following technological progress in microfabrication,[6–8] a branch of microfluidics that involves emulsions has been growing for the last ten years.[9–16] The enthusiasm for droplet-based microfluidics has spread mainly because it is possible to form and to manipulate calibrated emulsion drops at a high rate. Easily accessible soft lithography techniques[6] have also contributed to the popularisation of microfluidics. This novel technology opened the way to revisit the concept of compartmentalisation in droplets[17] where emulsion droplets act as small test tubes in which biological activities[18] or chemical reactions[19] take place in a more controlled manner.[20–24] In addition, the handling of thousands of those microreactors, whose composition can be continuously tuned, leads to high throughput applications.[25–34] Finally, microfluidics allows finely designed complex emulsions such as multiple-emulsions, core–shell or janus structures that ultimately lead to a highly efficient encapsulation of active compounds or to calibrated and tailored particles.[35–38]

Besides these applications, microfluidic technology offers a powerful tool for investigating the properties of emulsions themselves, as was recognised a few years ago. This is the heart of the present review, which is developed as follows. In the first section, the various ways to form calibrated emulsion droplets in microfluidic systems are briefly described with particular attention on the creation of drop pairs that enables exploration of the destabilisation mechanisms of emulsions at the level of two drops. Then, in a second section, the use of microfluidics for characterising the interfacial properties of emulsions that are linked to their stability is discussed. A third section is devoted to the coalescence of droplets that are either forced, under flow or under electric field, or thermally activated. A fourth section is dedicated to the diffusion of molecules between droplets through surfactant monolayers and *via* the continuous phase or through surfactant bilayers. The microfluidic tool is well suited for investigating such phenomena since it enables decoupling of the formation and the destruction steps of an emulsion, to

manipulate many individual droplets and to monitor finely the interaction between them.

II. Emulsification

A. Calibrated drops

Emulsification based on a mechanical process follows the paradigm of liquid fragmentation, *i.e.* droplets result from the breakup of a liquid finger or jet,[39] in the same way as spray formation. The destabilisation of a liquid column driven by surface tension[40,41] leads ultimately to the formation of a collection of droplets characterised by a size distribution that is mainly governed by the fluid interface roughness.[42] This roughness has multiple origins and may be a consequence of turbulence, for example. To summarise, the more corrugated a liquid ligament is, the wider a drop size distribution is and *vice versa*. Several techniques have been developed for making emulsions[1] and they mostly rely on shear induced breakup.[43] In that case, large drops are elongated under flow until they form a liquid ligament that divides into smaller drops through a capillary instability. Moreover, the final size distribution is shaped by a competition between drop breakup and drop coalescence. An emulsion can also be obtained by flowing a liquid through an orifice, or many in the case of a membrane,[44] into a bath containing a second liquid at rest or under flow. When a liquid finger emerges from a hole, the interfacial tension can prevent the formation of a liquid jet. Instead, a growing drop is connected to the orifice wall by a liquid bridge that finally pinch-off because of surface tension. Bulk or membrane emulsification leads to broad distributions of droplet size (Fig. 1) since the main parameters that control the drop formation, such as the shear or the membrane pore size, are not homogeneous.

It has been demonstrated that a controlled shear over all the emulsion that is confined in a small gap can lead to monodisperse droplets.[45] Also, flowing two immiscible fluids through a small aperture in a thin plate or a narrow capillary gives rise to a fine laminar jet that produces calibrated droplets[46,47] or bubbles.[48] Finally, drops can be torn off one-by-one at the end of a needle owing to the co-flow of the continuous phase.[49] Thanks to microfluidic technologies, the aforementioned mechanisms of emulsification have been exploited for making droplets in a more controlled way.[50] The formation of a regular droplet train is obtained by flowing two immiscible liquid streams through three main geometries: cross-flowing (Y or T junctions),[51] co-flowing[52] and flow focusing.[53] For the cross-flow configuration, inspired by analytical chemistry applications,[54] two modes of drop formation occur: either the drops are broken off *via* the shear stress imposed by the carrier fluid or as a result of the confinement.[55] For the later mode, a high pressure is built up once the dispersed phase invades most of the cross-section that confines the flow of the carrier fluid in the lubricating film along the wall. This ultimately leads to a periodic pinch-off of the invading liquid finger and therefore to monodisperse droplets.[56] This mode of drop formation, that is a direct consequence of the confinement, takes also place in the two other geometries and is a signature of an absolute instability.[57] A transition between a dripping regime, where drops are directly formed at the end of the injection tube or channel of the dispersed phase, and a jetting regime also occurs,[58] in a similar way to an unconfined situation.[59] For the latter condition, since the drops stemmed from the instability of a liquid cylinder, the fragmentation is more sensitive to noise that induces a size polydispersity. To circumvent this issue in rectangular channels, an ingenious strategy is to increase the vertical confinement in order to form a squeezed jet that is stable[60–62] and then to trigger the break-up of such a liquid tongue by a sudden expansion of the channel height[62–64] or width.[62] This is a follow up to a membrane emulsification process that has been upgraded by using micro-machined pores with a terrace at the pore exit that also induces a pinch-off of the liquid stream driven by surface tension.[65]

To conclude, there are many microfluidic ways to form calibrated emulsion droplets with sizes ranging from a micrometer to a few hundreds of micrometers with a production rate, obviously linked to droplet size, varying from a few Hz to more than ten kHz.[64] One of the main outcomes from following such a microfluidic route is the ability to uncouple the formation and the destruction steps of an emulsion. A next step is then to be capable of forming drop pairs in order to probe the interaction between drops at the level of two objects.

B. Drop pairs

Investigations on emulsion stability mainly rely on bulk experiments that usually lead to average measures. Moreover, phenomena that occur at a mesoscopic level, *i.e.* at a drop scale, are difficult to monitor. There exist methods to probe the interaction between two emulsion drops, such as four roll mill apparatus,[71] dual micropipette set-ups[72,73] or optical vortex trap techniques[74] but reliable statistical analyses are laborious to obtain. This issue is easily circumvented by employing a microfluidic strategy.

The break-up of droplets occurring at a T-junction[75] can be exploited for making pairs of identical droplets once a loop is implemented[66] as shown in Fig. 2(a). The use of a slightly asymmetrical loop allows the delay of one droplet with respect to the other and thus to avoid collision at the exit of the loop. Then, before a drop collision is induced by a widening of the channel, the distance between the two droplets can be adjusted by removing or adding part of the continuous phase.

To make binary pairs, *i.e.* where the composition of each drop is different, two drop formation modules are necessary and a synchronisation is required. An alternating drop formation can be obtained by simply coupling the drop makers through the continuous phase whatever the geometry, *i.e.* T-junction[67,76–78] (Fig. 2(b)), flow focusing[78,79] or step.[80] Because of this hydrodynamic coupling, inherent flow rate fluctuations and channel size imperfections, the dual drop formation exhibits a rich dynamical behaviour. The fragmentation can be synchronised, either in phase or out of phase, quasiperiodic or chaotic.[81] A key point for a successful synchronisation is to produce droplets larger than the channel size in order to alter efficiently the continuous flow.[81] Synchronised drop production by using an electrical coupling has been recently demonstrated[82] as well as *via* electrowetting that allows the control of drop production on-demand.[83,84]

Next, to probe the interaction between two binary droplets, pairs have to be isolated. This segregation can be obtained under flow by working with a dilute emulsion. This is simply achieved

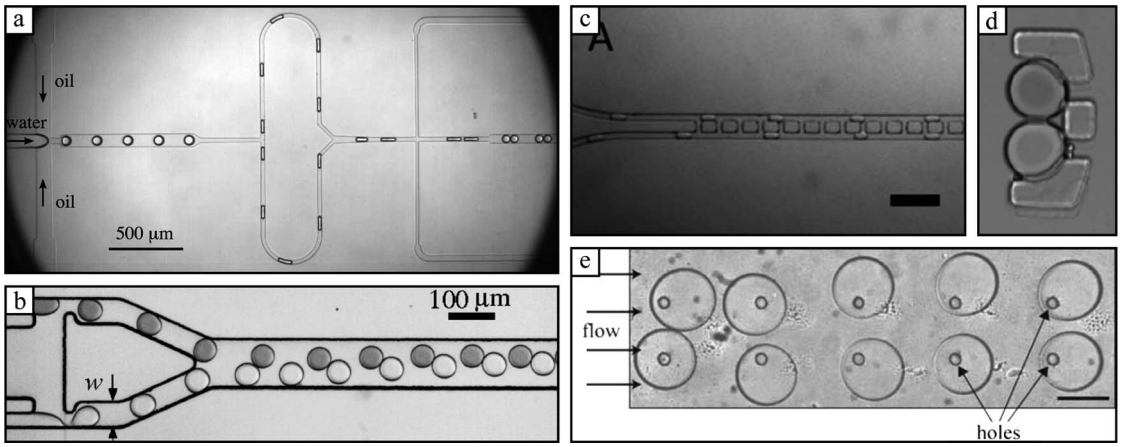

Fig. 2 Formation of droplet pairs under flow and at rest. (a) Train of identical droplet pairs from splitting at the entrance of a loop. Reproduced with permission from ref. 66. Copyright (2008) by the American Physical Society. (b) Train of binary droplets from coupled droplet generators. Reprinted with permission from ref. 67. Copyright (2008) American Chemical Society. (c) Synchronisation of two streams of droplets with the help of fluid bypasses. Reproduced from ref. 68. (d) Parking of a droplet pair into a well. Reprinted with permission from ref. 69. Copyright (2011) American Chemical Society. (e) Trapping of drops *via* localized surface energy lowering induced by holes on the channel wall. Reproduced from ref. 70.

by increasing the flow rate ratio between the continuous phase and the dispersed phase prior to drop formation and by flowing a stream of the carrier liquid after drop production. Finally, the pairing can be induced by an expansion of the lateral channel size[85,86] or an array of lateral pillars,[87] by a drop size difference that leads to a velocity contrast[88] or by again coupling the two drop trains[68,89] with the help of bypasses[90] as shown in Fig. 2(c).

Monitoring the stability of drop pairs under flow is limited to short timescales. Therefore, for long duration experiments, drops must be trapped for overcoming this restraint. A first strategy is to generate a train of drops, or alternative drops, and to let them flow in an array of small wells where only two drops fit, as in ref. 69, 91 and 92 inspired from cell trapping devices.[93] An example is reported in Fig. 2(d). A more efficient way for trapping binary pairs is to use a double trap system.[94] Another ingenious way is to take advantage of the vertical confinement of microchannels that allows the holding of captive droplets *via* a local interfacial energy lowering induced by a simple hole that can be much smaller than the drop size[70] (Fig. 2(e)).

III. Interfacial properties

The interfacial properties of an emulsion play a major role all along their lifetime, from their creation to their destruction. Knowing such properties is therefore crucial for understanding and controlling their stability.[95,96] There are well established techniques for measuring the interfacial tension between liquids,[97] where kinetic adsorption of surface active agents can be monitored, as well as the rheological properties of the interfaces.[98,99] What are the benefits of using microfluidics to evaluate interfacial properties? A first advantage is the ability to probe large surface-to-volume ratios as it occurs in real systems and is not available from common macroscopic techniques. This is convenient since drop size rules the surfactant mass transfer mechanisms,[100] *i.e.* kinetically or diffusion controlled. Working with small drops leads to faster equilibrium dynamics. Moreover, handling micrometric droplets can limit the role played by impurities that may be present in the dispersed phase and that cannot be purified, when natural oils or bio-synthesised surfactants are investigated,[15] for instance. Another benefit inherent to microfluidics is the possibility to screen formulations.

A straightforward way to measure the interfacial tension is to extend the drop volume technique, where gravity drives the formation of drops against surface tension, to a microfluidic system where the shear is responsible for emulsification. Whatever the geometry of drop formation, either co-flow[101] or cross-flow,[102,103] this technique requires a calibration step. Moreover, since the method is based on small drop formation, only short time scales on the order of the millisecond are accessible. Therefore, most of the measurements are realised far from equilibrium.

Hudson and collaborators developed a microfluidic strategy for assessing interfacial properties from droplet shape distortion and internal flow field.[104] The evaluation of the interfacial tension γ in a microfluidic system[105] is based on the droplet deformation in an extensional flow field (Fig. 3(a)) that has been theoretically described by Taylor.[43,106] The deformation amplitude is almost independent of the viscosity ratio between the two liquids and depends linearly on the capillary number $C_a = \eta_c R\dot{\varepsilon}/\gamma$, where η_c is the continuous phase viscosity and $\dot{\varepsilon}$ is the extension rate. A demonstration of such a procedure has been conducted on drop sizes ranging from 9 μm to 220 μm and surface tensions varying from 2.5 mN m^{-1} to 60 mN m^{-1} (ref. 105) and by modifying the drop composition on the chip.[107] The ageing of the interface can in principle be evaluated by implementing a series of

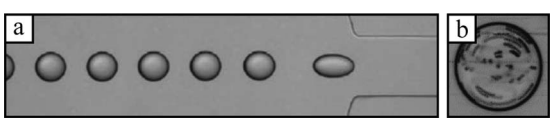

Fig. 3 Evaluation of interfacial properties *via* (a) the drop deformation induced by the flow into a microchannel constriction. Reproduced from ref. 107. (b) The internal flow generated by the external flow as revealed by the presence of particles. Reproduced from ref. 104. Copyright (2011) Wiley-VCH Verlag GmbH & Co. KGaA.

constrictions along the microchannel.[105] Finally, the mobility of the interface, *i.e.* the surface velocity, can be assessed *via* the visualisation of the flow inside the drops by using a particle tracking technique[108] (Fig. 3(b)) combined with a theoretical description of the internal flow field.[109,110]

The use of the electrowetting phenomenon[111] can help to probe the interfacial tension of small drops, down to a radius of 170 μm for a sessile drop on a planar electrode[112] or sandwiched between two planar electrodes with an interstice of 100 μm.[113]

Nowadays, the microfluidic strategies for assessing interfacial properties are mainly restricted to the interfacial tension. The rheological features of liquid interfaces, which are difficult to access, are crucial for understanding and controlling emulsion stability.[95] Therefore, the next challenging step is to invent microfluidic routes for evaluating the frequency dependence of interfacial viscoelastic properties of emulsion droplets as well as their ageing mechanisms. Electro-actuation may be a good candidate for achieving these characterisations.[114]

IV. Coalescence

The scenario of drop coalescence can be divided in three main parts. First, the liquid between two drops is drained out thanks to external flow, buoyancy or Brownian motion depending on the drop size and volume fraction. This hydrodynamic step is sensitive to boundary conditions and thus to interfacial properties dictated by the nature and the spatial distribution of surface active agents at the interfaces.[115,116] Indeed, a surface concentration gradient of surfactant molecules leads to a surface tension gradient and thus to a stress at the interface opposed to the flow, namely the Marangoni effect. Then the interstitial film thins until the two interfaces interact *via* surface forces. When only van der Waals forces are acting, and since they are attractive in such a symmetric system, the film draining is hastened and thermal fluctuations of the interfaces may be amplified.[117–119] An equilibrium thickness is reached when repulsive forces, such as electrostatic or steric forces, are present.[95] The last step is a thermally activated process that consists of the nucleation of a pore in the thin film that bridges the two adjacent droplets.[120] The pore may reach a critical size above which it becomes unstable and grows leading to the fusion of two droplets.[121,122] There are two regimes of coalescence that depend on the amplitude of the activation energy for nucleating an unstable pore. For clean interfaces or for low surface coverage of surfactants, the energy barrier is so weak that the overall process is principally ruled by hydrodynamics. In that case, the lifetime of a droplet pair is dictated by the time needed for approaching the two drop surfaces close enough for coalescence to be nucleated. On the other hand, for larger surfactant coverage, and thus for higher energy barriers, the thin film is metastable and may last months before a sufficiently large pore is nucleated through thermal fluctuations of the surfactant surface concentration.[123–125]

From an experimental point of view, the detailed observation of drop or bubble coalescence has been made feasible thanks to the development of high speed imaging technologies.[126] Moreover, microfluidic devices are generally two-dimensional networks of channels having a height of the order of the drop size. Thus, the combination of the imaging and the microfluidic capabilities allow fine probing of the droplet coalescence phenomenon at the scale of a droplet. Finally, the possibility to form calibrated droplets at a relatively high rate opens the way to conduct statistical analyses of droplet coalescence which are not accessible in bulk experiments.

The distinction between the two regimes of coalescence, named forced and activated, is linked to the dominant process: either the coalescence is governed by the dynamics for approaching the drop surfaces or it is ruled by thermal fluctuations at the liquid interfaces. The two following subsections are dedicated to forced coalescence, *i.e.* where the energy barrier to fusion is weak. Studies on activated coalescence are then reported in a third subsection.

A. Hydrodynamical forcing

The stability of an emulsion under flow can be assessed by inducing collisions of droplets among a droplet train following a widening of the channel.[128] Baret *et al.* quantified the stability of an initially monodisperse emulsion by measuring the drop size distribution at the end of the colliding chamber. They determined the probability to coalesce as a function of surfactant concentration and the delay time between the drop formation and their collisions. They confirmed that the adsorption kinetics of surfactant molecules at liquid interfaces rules emulsion stability at short times. This approach has been extended to more complex interfaces where peptides,[129] polymers[130] or colloids[131] were present. The details of the collision between droplets, that are known to play a crucial role in the coalescence process *via* the draining dynamics of the continuous phase between drops,[71,116,132] were not considered. This aspect has been recently investigated in a free surfactant system.[133] Krebs *et al.* analysed the erratic collisions of thousands of drops and were able to estimate the distribution of the coalescence time t_c as a function of drop size, volume fraction and impact velocity. Since for this system without surfactant the energy barrier to ultimately merge two droplets is nearly zero, the coalescence process is deterministic and the fusion time distribution can be attributed to drop size distribution and flow fluctuations. They corroborated the fact that the mean value of t_c is a decreasing function of the drop size and the impact velocity.[71] On the other hand, the scaling of t_c does not match the one of three dimensional experiments since the vertical confinement strongly influences the hydrodynamics of droplets[134] and their coalescence.[135]

Using an adequate channel design, the collision of isolated droplet pairs can be controlled.[66] Bremond *et al.* demonstrated that when two droplets collide and then move away from each other, the coalescence is more probable during the separation phase (Fig. 4(a)). This counterintuitive phenomenon has been mentioned by Loewenberg and Hinch[136] from boundary integral simulations and scaling arguments that describe drop collision in a shear flow where drops can merge in the extensional quadrant *i.e.* when drops are pulled apart. This has been then observed in experimental studies using a four-roll mill device[71,137,138] and confirmed by numerical simulations.[139] The underlying mechanism is the pressure reduction in the interstitial film between the two drops when they are pulled apart and that induces a bulging out of the interfaces.[71,140,141] Because of these facing deformations, the two interfaces get locally closer allowing coalescence to

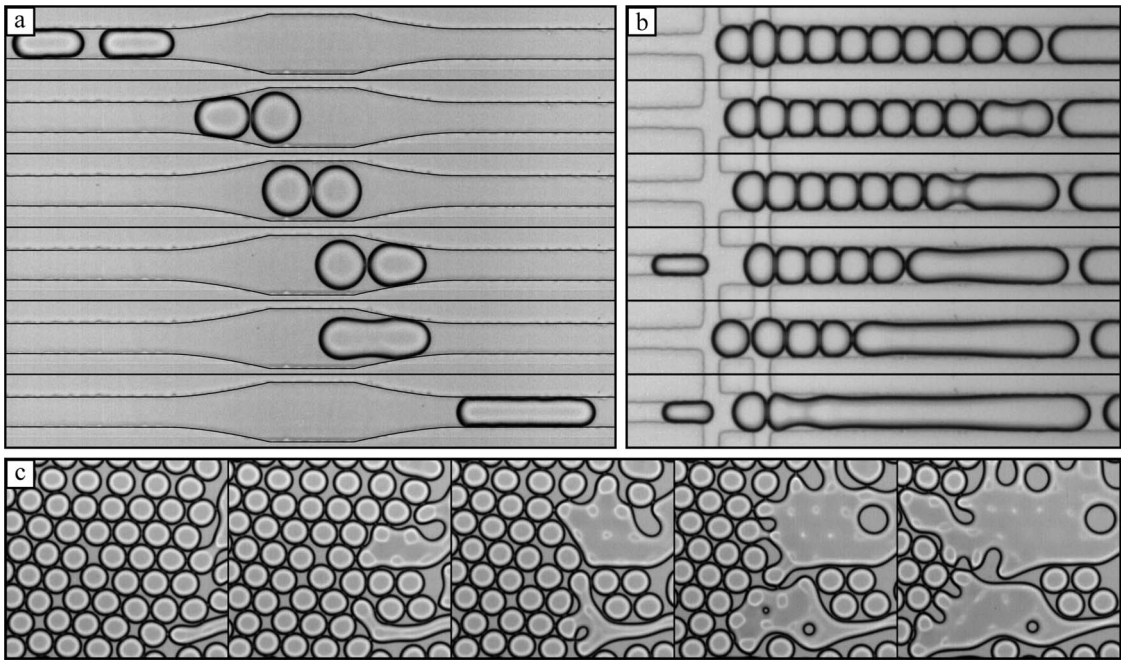

Fig. 4 Separation-induced coalescence. (a) Collision and separation of two droplets demonstrating that coalescence is favoured when droplets are pulled apart. Reproduced from ref. 66. Copyright (2008) by the American Physical Society. (b) Cascade of coalescence events in a compact train of droplets where the interfacial tension, that induces drop shape relaxation and thus separation with neighbouring drops, is the motor of the propagation. Reproduced from ref. 66. Copyright (2008) by the American Physical Society. (c) Propagation of coalescence among a concentrated two-dimensional emulsion that may lead to phase inversion. Reproduced from ref. 127. Copyright (2011) by the American Physical Society.

be nucleated. One may note that among the three possible outcomes of the collision of two droplets at a T-junction,[142] merging, splitting and slipping, the regime named "late coalescence" where the drops fuse in the outlet channel arises from the same mechanism. It is also worth to mention that the bulging out of elastic surfaces embedded in a liquid[143] or liquid interfaces[144] has also been noticed in experimental studies based on surface force apparatus when the two surfaces are moving away from each other. Despite a sign error in the expression of the curvature that invalidates the analytical model of Lai *et al.*, their scaling argument remains correct.[140] For a no-slip boundary condition, the deformation amplitude $\tilde{h}$ is expected to be $\tilde{h} \sim \eta_c \dot{h}_0 R^2/\gamma h_0$, where η_c is the continuous phase viscosity, γ is the interfacial tension, R is the drop radius, h_0 is the minimal separation distance between undeformed droplets and $\dot{h}_0 = \mathrm{d}h_0/\mathrm{d}t$ is the separation rate. Coalescence may occur if $\tilde{h}$ is of the order of h_0, as confirmed when coalescence time is considered.

Maybe more importantly, Bremond *et al.*[66] shown that such a separation-induced coalescence is then responsible of the propagation of coalescence among a compact train of droplets (Fig. 4(b)). Here, the interfacial tension is the motor of the propagation. Indeed, the shape relaxation during coalescence spontaneously results in a separation with the neighbouring drops, a situation that is potentially destabilising. The coalescent nature of coalescence, that has also been reported in other microfluidic studies,[145–147] is believed to be responsible of catastrophic destruction of concentrated emulsions under shear that might undergo phase inversion. This assertion has been demonstrated in a two-dimensional emulsion by using a microfluidic approach[127] as reported in Fig. 4(c). Since the coalescence of two drops leads to a non isotropic flow[148] and because the deformation amplitude of the interstitial film depends on the rate of retraction,[140] the probability that the merging of two drops triggers the coalescence of a third drop is a function of the angle between drops.[127] Thanks to the large number of events that can be monitored in a microfluidic experiment, the probability to coalesce P_c was efficiently evaluated. The coalescence probability is maximum for aligned drops and then decreases to zero for angles larger than 130°. Then, the probability that phase inversion occurs, *i.e.* when the fusion of neighbouring drops leads to the entrapment of the continuous phase, can be inferred from P_c. Moreover, it was predicted that polydispersity should favour phase inversion, an assertion that needs to be experimentally demonstrated. Finally, enough surfactant has been added for preventing fusion during the compaction of the emulsion but did not prevent the propagation of coalescence where the local deformation of droplet interface might have swept away the surfactant and therefore promoted fusion.

B. Electrodynamical forcing

The use of an electric field is widely used for inducing coalescence of water-in-oil emulsion drops in oil recovery applications[149] or droplet-based microfluidics,[88] for instance. The electro-coalescence phenomenon is based on three main mechanisms: two neighbouring drops experience a dielectrophoretic force that drives them toward one another;[150] because of the heterogeneity of the electrical stress the interfaces are deformed and thus come closer;[151] and finally the activation energy for coalescence is lowered.[152] The last point will be discussed in the next section. A

water drop, that is usually a conductive medium, immersed in a dielectric medium of dielectric constant ε_c and subjected to an uniform electric field E_0 is polarised and generates an electric field in a similar way to a dipole source.[153] The resulting anisotropic electrical stress σ_E built up at the water–oil interface, that scales as $\sigma_E \sim \varepsilon_c \varepsilon_0 E_0^2$, is responsible for a drop shape transition from a sphere to a prolate spheroid.[151] The drop can then undergo disintegration once the electrical stress overcomes the restoring capillary pressure $p_c \sim \gamma/R_0$ by forming thin jets at both poles that break up into micron size droplets.[154–156] If a second drop is in the vicinity of the first one, the electric field at the surface of the drops is amplified because of dipole–dipole interaction and becomes stronger as they come closer.[157] Therefore, the drop pair can be destabilised at lower E_0, as has been demonstrated for drops in air.[158] For closed drops at a fixed potential, the critical potential above which drops merge depends linearly on the ratio between drop separation and drop radius.[159,160] For emulsions, because traces of charges are frequently present in the oil phase, this later one cannot always be regarded as a perfect dielectric and a leaky dielectric model must be considered.[161–163]

Electrodes can be easily implemented in a microfluidic device. Flat electrodes, that generate inhomogeneous electric fields, are made by vapour deposition combined with photolithography or electron beam lithography techniques. A more homogeneous electric field throughout the channel height is obtained by directly casting the electrodes.[165] High electric field intensities are thus accessible in microsystems. Employing a microfluidic strategy for the investigation of electrocoalescence enables easy variation of the drop size and the distance between them, as well as the field strength. Following this route, Thiam *et al.* mapped out the stability diagram of a droplet pair under an ac electric field that leads to ionic polarisation of the droplets.[164] As reported in Fig. 5, they found three different regimes: stable, coalescence and partial merging. The frontier separating stable and unstable pairs remains essentially the same for different dispersed phase conductivities σ_d and follows qualitatively the same trend as previously observed and predicted for a system made of water drops in air,[158] *i.e.* the closer the drops are the lower the critical electric field strength is, thanks to the enhancement of the electric field at the two facing poles. For the partial merging region found beyond a critical relative drop separation, the interface instability can lead to two different behaviours depending on σ_d and the electric field frequency f. When $1/f$ is larger than the characteristic time $\tau_r = \varepsilon_d/\sigma_d$, related to the bulk charge relaxation in the dispersed phase, the liquid bridge that links the two drops breaks *via* a capillary instability[166] and the two drops repel each other under field thus revealing a charge exchange during the partial fusion.[167,168] By contrast, for $f\tau_r > 1$, a thin and stable bridge is observed. The stabilisation of the liquid thread may arise from mutual Coulombic repulsion between the free charges at the interface.[169,170] These two different behaviours then impact on the whole destabilisation of a collection of drops. Indeed, for $f\tau_r < 1$ the interaction between drops is ruled by a two-body interaction, *i.e.* adjacent droplets merge only if they are close enough whatever the field strength; for $f\tau_r > 1$, the coalescence propagates even for a high drop separation thanks to the stabilisation of the liquid bridge.[164] Szymborski *et al.* used a wide microfluidic chamber for studying the effect of the electric field frequency and intensity along with the amount of ions in the dispersed phase on the destabilisation of a two-dimensional emulsion.[171] Without considering the drop separation distance, they observed that the critical electric field amplitude above which coalescence occurs increases with f and decreases with the ion concentration. They suggested that the ionic mobility modifies the ionic polarisation of the drop surface and thus the electrocoalescence process.

The electrocoalescence phenomenon has also been investigated at the level of a single interstitial film in a microfluidic system where two liquid fingers whose electrical potential and separation distance could be tuned.[172] The authors observed a linear dependence between the critical potential that leads to coalescence and the film thickness, as expected by Taylor's analysis.[159]

For microfluidic application purposes, drops must be close enough for ensuring an efficient fusion under electric field. This can be obtained by holding a first droplet with flow bypasses[173] or patterned electrodes under the microchannel,[174,175] the droplet being trapped thanks to dielectrophoretic forces,[176] which then coalesce under field with a second moving droplet.

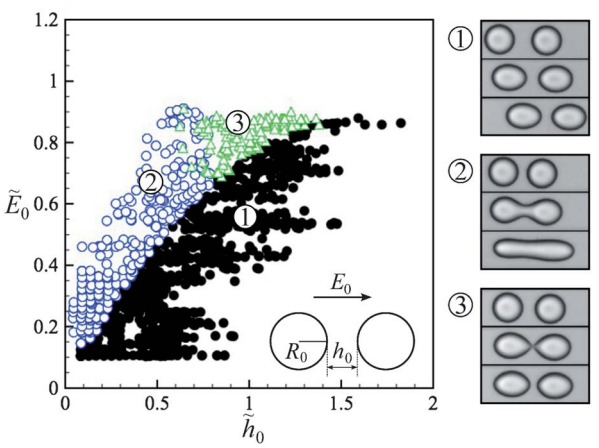

Fig. 5 Phase diagram of two water drops initially separated by $\tilde{h}_0 = h_0/R_0$ and subjected to an ac electric field $\tilde{E}_0 = E_0(\varepsilon_c \varepsilon_0 R_0/\gamma)^{1/2}$ at 10 kHz. Three states of the drop pair are found: (1) stable (●); (2) unstable with coalescence (○); (3) unstable with partial coalescence (△). Adapted from ref. 164. Copyright (2009) by the American Physical Society.

C. Activated coalescence

Emulsions are known to become adhesive and thus lead to the formation of a surfactant bilayer between adjacent drops.[3] Adhesion is initiated when an ionic surfactant in combination with salt is used in direct emulsions[177,178] and by decreasing the solvent quality for surfactants in the case of inverse emulsions.[179] The later case allows mimicking of vesicle membranes.[180] Similar to a wetting phenomenon, the contact angle θ between two adhesive drops directly reflects the adhesion energy $\Delta F = 2\gamma_0(1 - \cos(\theta))$, where γ_0 is the surface tension between water and oil with amphiphilic molecules (Fig. 6(a)). For inverse emulsions, the adhesive energy can be modified by using an oil mixture,[179] one being a poor solvent for surfactants, and by tuning the oil composition. The surface pressure $\Pi = \gamma_0 - \gamma_m$, where γ_m is the

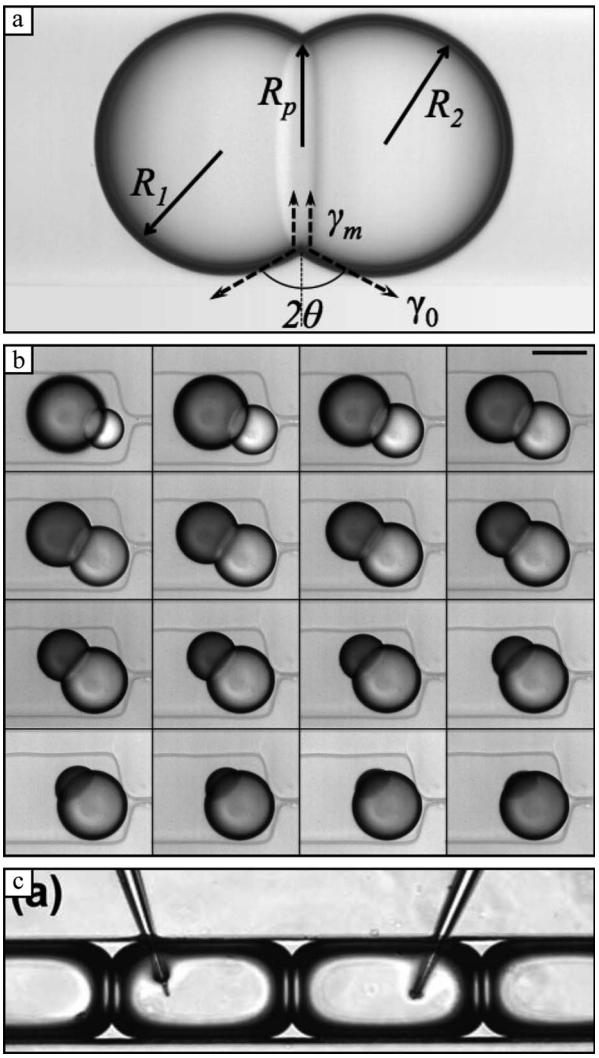

Fig. 6 (a) Snapshot of two adhesive water-in-oil drops forming a surfactant bilayer between them along with the main parameters of the drop pair. Reproduced from ref. 91. Copyright (2011) by the American Physical Society. (b) Time sequence showing the transport of water between two adhering drops having different compositions and from which the permeability of the bilayer can be assessed. Reprinted with permission from ref. 92. Copyright (2012) American Chemical Society. (c) Implementation of two electrodes made of micro-pipettes used for investigating the electroporation process of the membrane separating adhesive droplets. Reproduced from ref. 191.

surface tension of a monolayer forming the bilayer, acting on the monolayer is simply $\Pi = \Delta F/2$. Therefore, the two-dimensional bilayer equation of state $\Pi(\Gamma)$, where Γ is the surfactant surface density which is controlled by solvent composition, can be assessed. Well known gas–liquid and liquid–gel transitions occurring in phospholipid monolayers[181] have been observed in the bilayer.[91,92]

The stability of such bilayers has been determined by Thiam *et al.* where adhesive pairs of inverse emulsion droplets were formed and trapped in microfluidic systems.[91,92] One of the major advantage to use microsystems as compared to bulk emulsions is the ability to form isolated adhering drop pairs where the contact angle θ is easily measured. For a given oil composition, there is a critical phospholipid concentration below which drops start to coalesce whereas they can last for days for large amount of surfactant. Below the critical concentration, either the drops coalesce while the adhesive patch is being formed or they fuse after the equilibrium angle has been reached. The first regime, when the surfactant coverage is dilute, may reflect a competition between patch growth and transport of phospholipids towards the adhesive region. In the second regime, there exists a probability P_c to coalesce that increases exponentially with time t, *i.e.* $P_c = 1 - \exp(-t/\tau_c)$. This feature is reminiscent of a nucleation process as it can occur in foam bilayers for low surfactant concentrations.[123] The mean lifetime τ_c of the bilayer is linked to the activation energy barrier that must be overcome to nucleate an unstable pore into the membrane.[121,123]

Under electric field, three distinct states were observed as a function of the adhesion energy and the electric field intensity. The pair can be either stable, though slightly deformed, or unzip and separate, or coalesce.[91] The unzipping frontier directly reflect vesicle detachment forces.[182–184] The drops repel each other after unzipping under field and can attract each other when the electric field is turned off. This is a signature of the electroporation phenomenon where transient pores are nucleated under field[152] and allow charge exchange between the drops that finally acquire a net charge. The coalescence frontier also reveals an electroporation process where the creation of a pore of radius r in a membrane of thickness h is associated with a free energy $\Delta W = 2\pi\Gamma r - 2\pi\gamma_m r^2 - 0.5\pi C_m h^2 E_m^2 r^2$.[152] The first term is the energy increase due to the line tension Γ which is almost constant as it depends essentially on the membrane's thickness.[2] The second term represents the energy decrease due to a reduction of the surface area. The last term, ΔW, comes from the accumulated energy of the membrane which behaves as a capacitor where C_m is the capacitance of the pored membrane and E_m is the local electric field proportional to the external electric field E_0.[152,185] The critical free energy of the pores under electric field that leads to the bilayer rupture is observed to be constant[91] and, according to the thermally activated mechanism of pore nucleation,[121] should be on the order of the thermal energy kT. Finally, for weak adhesion energy, *i.e.* in the gas phase where the bilayer is poor in surfactants, coalescence occurs before drops are able to detach and thus precludes any unzipping of the bilayer.

A common technique for investigating the stability of thin films, foams or emulsions, is the so-called thin film balance initially used for surface force measurement.[186] Following previous miniaturizations of the cell for making suspended thin liquid films[187,188] in order to reach the film size of usual emulsions, Mostowfi *et al.* developed a microfluidic system for making single emulsion films with a lateral size around 10 micrometers.[189,190] They were able to correlate the critical potential difference above which rupture of the thin film occurs and the kinetics of surfactant adsorption.

V. Permeation

An emulsion involves *a priori* two immiscible liquids but mass transfer between drops does usually exist. This molecular diffusion occurs because of a finite solubility of each phase into each other and also because surfactant micelles can act as cargo for molecular transport that ultimately increases solubility.[4]

Chemical potential heterogeneity among the emulsion is the driving force of such a molecular transfer. For emulsion drops having the same composition, the chemical potential mismatch arises from the drop size distribution that leads to a distribution of the capillary pressure. This results in the growth of large drops at the expense of smaller ones, a phenomenon named Ostwald ripening.[4,192] Obviously, a flux of molecules is initiated between drops once their composition is not homogeneous among the whole system in order to balance chemical potentials. This phenomenon has been exploited for screening protein crystallisation conditions[193] or for monitoring the bioactivity of microorganisms as well as an enzymatic reaction that takes place in water-in-oil emulsion droplets that were formed, immobilised and sampled in a microfluidic device.[194,195]

The dissolution of droplets in a dilute emulsion has been quantified with the aim to concentrate solutes that cannot escape from the aqueous compartment.[196] It has been observed that the use of microchannels made in PDMS led to a high dissolution rate as compared to polystyrene, since many molecules easily diffuse through PDMS.[197] The permeability of PDMS to water has been used to evaluate the phase diagram of multicomponent fluid mixtures contained in droplets.[198,199] One may also take advantage of the large surface-to-volume ratios involved in microfluidic droplets for enhancing liquid–liquid extraction.[200–202] For moving droplets, convection can dominate diffusion, *i.e.* for a high Peclet number defined as $P_e = UR/D$ where U is the characteristic droplet velocity, R the droplet size and D the diffusion coefficient. In that case, the amount of matter transferred across the droplet interface grows as the square root of time and the time it takes for the transfer process to be completed decreases as $P_e^{-2/3}$.[202,203] The mass exchange between binary droplets has been monitored in a two-dimensional emulsion stored in a microfluidic chamber.[204] An adequate formulation has been found for preventing any leakage of entrapped molecules into the droplets whose transport was assisted by surfactant micelles.

Adhesion can promote a faster matter exchange[191,195] since the neighbouring drops are separated by a thin membrane having a thickness δ of a few nanometers[179] such as the so-called Newton black film occurring in foams.[123] Indeed, according to the solubility-diffusion mechanism,[205] the permeability P_m of the membrane, which relates the flux of molecules through the membrane and the osmotic activity gradient, is $P_m = KD_m/\delta$ when the rate-determining step is diffusion in the membrane. Here, K is the partition coefficient of the diffusing molecules characterised by a diffusion coefficient D_m in the membrane. By making binary adhesive drops in a microfluidic device, one class of drops were composed of pure water and the second one contained electrolytes; the permeation kinetic of water molecules through the adhesive bilayer has been monitored as a function of the continuous phase composition.[92] An example of water exchange among a binary pair is reported in Fig. 6(b) where a pure water droplet (labelled with methylene blue dye) adheres to a droplet containing 150 mM of $MgSO_4$. Since water molecules can diffuse faster through the bilayer than electrolytes, a flux of water is set between the two droplets in order to balance chemical potentials. This work confirmed previous observations on vesicle permeability to water that is correlated to the membrane fluidity,[206] but with a better control of bilayer properties that are here tuned by the oil mixture composition.

As previously discussed, one can permeabilise bilayers to enable the transport of large molecules or electrolytes by using an electric field.[152,207] The electroporation process of a surfactant bilayer between adhering droplets has been monitored by implementing microelectrodes in a PDMS microchannel as shown in Fig. 6(c).[191] The ionic conduction current, when short voltage pulses with an amplitude U were used, is well accounted for by electroporation theory that predicts a rate of nucleation of transient pores to scale like $\exp(U^2/kT)$.[208] Transmembrane proteins, that act as an ionic channel through the membrane, can also be incorporated *via* the aqueous phase.[191] A few procedures have been designed for making artificial bilayers in microfluidic systems[209] in order to study the function of membrane proteins. For example, a bilayer can be formed by the meeting of two water-in-oil fingers at a cross junction[210] or, as previously discussed, by manipulating pairs of water-in-oil emulsion drops.[211]

VI. Conclusion and perspectives

Microfluidic technology offers new opportunities to investigate emulsion properties and behaviour. Indeed, some aspects of their phenomenology have remained quite unexplored, and almost impossible to access. This is mainly due to the fact that in the conventional batch format the time it takes to produce the emulsion remains on the order of several minutes, precluding any characterisation of shorter-timescale phenomena. Therefore, questions related to emulsion metastability, including coalescence and ripening, have been only partially answered. Emulsions with significantly long lifetimes have been intensively studied from various bulk approaches, mainly focusing on the thermally activated regime of coalescence, in agreement with Bancroft's empirical rules and its microscopic interpretation based on surfactant spontaneous curvature. Phenomena occurring much faster were therefore left out, until microsystems opened the route for decoupling preparation and destruction of such materials. Moreover, the use of ultrafast imaging allows today easy observation of submillisecond timescale processes. Microsystems also offer the possibility to impose very controlled flows and therefore apply to precise hydrodynamic conditions and constraints, which is extremely difficult to perform in a bulk system. This is a strong advantage which has led to the important discoveries reported in this review, and particularly the first possible scenario for explaining the well-known phase inversion ability of emulsions in presence of shear. The implementation of external electrical fields is also very straightforward, opening interesting conditions to revisit electrocoalescence and electroporation phenomena. A peculiar feature of microfluidic systems is the very high throughput rate production of droplets, droplets pairs, droplet trains, *etc*. This allows a large number of events to be analysed reliably, producing fast statistical data and thus an efficient mapping out of stability diagrams. More generally, the on-demand manipulation of droplets in microfluidic circuits offers a variety of unexplored configurations to be designed and studied. It is possible to rapidly screen formulations with fine tuning of the interface properties and to thus assess how it impacts on the emulsion stability. It is believed that microfluidic systems will become, if they are not already, the best route for characterising emulsions' properties as well as learning about their novel aspects.

References

1 F. Leal-Calderon, V. Schmitt and J. Bibette, *Emulsion Science – Basic Principles*, Springer, 2007.
2 B. Cabane and S. Hénon, *Liquides – Solutions, Dispersions, Émulsions, Gels*, Belin, 2007.
3 J. Bibette, F. L. Calderon and P. Poulin, *Rep. Prog. Phys.*, 1999, **62**, 969–1033.
4 A. Kabalnov, *J. Dispersion Sci. Technol.*, 2001, **22**, 1–12.
5 E. Dickinson, *Food Hydrocolloids*, 2003, **17**, 25–39.
6 Y. Xia and G. M. Whitesides, *Angew. Chem., Int. Ed.*, 1998, **37**, 550–575.
7 H. Becker and L. E. Locascio, *Talanta*, 2002, **56**, 267–287.
8 E. Verpoorte and N. F. De Rooij, *Proc. IEEE*, 2003, **91**, 930–953.
9 A. Gunther and K. F. Jensen, *Lab Chip*, 2006, **6**, 1487–1503.
10 S. Haeberle and R. Zengerle, *Lab Chip*, 2007, **7**, 1094–1110.
11 S. Y. Teh, R. Lin, L. H. Hung and A. P. Lee, *Lab Chip*, 2008, **8**, 198–220.
12 A. Huebner, S. Sharma, M. Srisa-Art, F. Hollfelder, J. B. Edel and A. J. Demello, *Lab Chip*, 2008, **8**, 1244–1254.
13 C.-X. Zhao and A. P. Middelberg, *Chem. Eng. Sci.*, 2011, **66**, 1394–1411.
14 H. Gu, M. H. G. Duits and F. Mugele, *Int. J. Mol. Sci.*, 2011, **12**, 2572–2597.
15 J. C. Baret, *Lab Chip*, 2012, **12**, 422–433.
16 R. Seemann, M. Brinkmann, T. Pfohl and S. Herminghaus, *Rep. Prog. Phys.*, 2012, **75**, 016601.
17 J. Lederberg, *J. Bacteriol.*, 1954, **68**, 258–259.
18 G. J. V. Nossal and J. Lederberg, *Nature*, 1958, **181**, 1419–1420.
19 B. Rotman, *Proc. Natl. Acad. Sci. U. S. A.*, 1961, **47**, 1981–1991.
20 H. Song, D. L. Chen and R. F. Ismagilov, *Angew. Chem., Int. Ed.*, 2006, **45**, 7336–7356.
21 D. T. Chiu, R. M. Lorenz and G. D. M. Jeffries, *Anal. Chem.*, 2009, **81**, 5111–5118.
22 A. B. Theberge, F. Courtois, Y. Schaerli, M. Fischlechner, C. Abell, F. Hollfelder and W. T. S. Huck, *Angew. Chem., Int. Ed.*, 2010, **49**, 5846–5868.
23 S. Vyawahare, A. D. Griffiths and C. A. Merten, *Chem. Biol.*, 2010, **17**, 1052–1065.
24 B. Kintses, L. D. van Vliet, S. R. A. Devenish and F. Hollfelder, *Curr. Opin. Chem. Biol.*, 2010, **14**, 548–555.
25 P. S. Dittrich, M. Jahnz and P. Schwille, *ChemBioChem*, 2005, **6**, 811–814.
26 L. Li, D. Mustafi, Q. Fu, V. Tereshko, D. L. L. Chen, J. D. Tice and R. F. Ismagilov, *Proc. Natl. Acad. Sci. U. S. A.*, 2006, **103**, 19243–19248.
27 M. M. Kiss, L. Ortoleva-Donnelly, N. R. Beer, J. Warner, C. G. Bailey, B. W. Colston, J. M. Rothberg, D. R. Link and J. H. Leamon, *Anal. Chem.*, 2008, **80**, 8975–8981.
28 J. Clausell-Tormos, D. Lieber, J. C. Baret, A. El-Harrak, O. J. Miller, L. Frenz, J. Blouwolff, K. J. Humphry, S. Koster, H. Duan, C. Holtze, D. A. Weitz, A. D. Griffiths and C. A. Merten, *Chem. Biol.*, 2008, **15**, 427–437.
29 F. Courtois, L. F. Olguin, G. Whyte, D. Bratton, W. T. S. Huck, C. Abell and F. Hollfelder, *ChemBioChem*, 2008, **9**, 439–446.
30 J. Hong, J. B. Edel and A. J. deMello, *Drug Discovery Today*, 2009, **14**, 134–146.
31 E. Brouzes, M. Medkova, N. Savenelli, D. Marran, M. Twardowski, J. B. Hutchison, J. M. Rothberg, D. R. Link, N. Perrimon and M. L. Samuels, *Proc. Natl. Acad. Sci. U. S. A.*, 2009, **106**, 14195–14200.
32 J. J. Agresti, E. Antipov, A. R. Abate, K. Ahn, A. C. Rowat, J. C. Baret, M. Marquez, A. M. Klibanov, A. D. Griffiths and D. A. Weitz, *Proc. Natl. Acad. Sci. U. S. A.*, 2010, **107**, 4004–4009.
33 L. Baraban, F. Bertholle, M. L. M. Salverda, N. Bremond, P. Panizza, J. Baudry, J. A. G. M. de Visser and J. Bibette, *Lab Chip*, 2011, **11**, 4057–4062.
34 O. J. Miller, A. E. Harrak, T. Mangeat, J.-C. Baret, L. Frenz, B. E. Debs, E. Mayot, M. L. Samuels, E. K. Rooney, P. Dieu, M. Galvan, D. R. Link and A. D. Griffiths, *Proc. Natl. Acad. Sci. U. S. A.*, 2011, **109**, 378–383.
35 R. K. Shah, J. W. Kim, J. J. Agresti, D. A. Weitz and L. Y. Chu, *Soft Matter*, 2008, **4**, 2303–2309.
36 W. Engl, R. Backov and P. Panizza, *Curr. Opin. Colloid Interface Sci.*, 2008, **13**, 206–216.
37 D. Dendukuri and P. S. Doyle, *Adv. Mater.*, 2009, **21**, 4071–4086.
38 S. Marre and K. F. Jensen, *Chem. Soc. Rev.*, 2010, **39**, 1183–1202.
39 J. Eggers and E. Villermaux, *Rep. Prog. Phys.*, 2008, **71**, 036601.
40 J. Plateau, *Statique expérimentale et théorique des liquides soumis aux seules forces moléculaires*, Paris, Gauthiers Villars., 1873.
41 L. Rayleigh, *Proc. London Math. Soc.*, 1878, **s1–10**, 4–13.
42 E. Villermaux, *Annu. Rev. Fluid Mech.*, 2007, **39**, 419–446.
43 G. I. Taylor, *Proc. R. Soc. London, Ser. A*, 1934, **146**, 501–523.
44 S. M. Joscelyne and G. Tragardh, *J. Membr. Sci.*, 2000, **169**, 107–117.
45 T. G. Mason and J. Bibette, *Phys. Rev. Lett.*, 1996, **77**, 3481–3484.
46 A. M. Ganan-Calvo, *Phys. Rev. Lett.*, 1998, **80**, 285–288.
47 I. Cohen, M. P. Brenner, J. Eggers and S. R. Nagel, *Phys. Rev. Lett.*, 1999, **83**, 1147–1150.
48 A. M. Ganan-Calvo and J. M. Gordillo, *Phys. Rev. Lett.*, 2001, **87**, 274501.
49 P. B. Umbanhowar, V. Prasad and D. A. Weitz, *Langmuir*, 2000, **16**, 347–351.
50 G. F. Christopher and S. L. Anna, *J. Phys. D: Appl. Phys.*, 2007, **40**, R319–R336.
51 T. Thorsen, R. W. Roberts, F. H. Arnold and S. R. Quake, *Phys. Rev. Lett.*, 2001, **86**, 4163–4166.
52 C. Cramer, P. Fischer and E. J. Windhab, *Chem. Eng. Sci.*, 2004, **59**, 3045–3058.
53 S. L. Anna, N. Bontoux and H. A. Stone, *Appl. Phys. Lett.*, 2003, **82**, 364–366.
54 B. Karlberg and S. Thelander, *Anal. Chim. Acta*, 1978, **98**, 1–7.
55 P. Garstecki, M. J. Fuerstman, H. A. Stone and G. M. Whitesides, *Lab Chip*, 2006, **6**, 437–446.
56 P. Guillot and A. Colin, *Phys. Rev. E: Stat., Nonlinear, Soft Matter Phys.*, 2005, **72**, 066301.
57 P. Guillot, A. Colin, A. S. Utada and A. Ajdari, *Phys. Rev. Lett.*, 2007, **99**, 104502.
58 A. S. Utada, A. Fernandez-Nieves, H. A. Stone and D. A. Weitz, *Phys. Rev. Lett.*, 2007, **99**, 094502.
59 C. Clanet and J. C. Lasheras, *J. Fluid Mech.*, 1999, **383**, 307–326.
60 Y. Son, N. S. Martys, J. G. Hagedorn and K. B. Migler, *Macromolecules*, 2003, **36**, 5825–5833.
61 B. Dollet, W. van Hoeve, J. P. Raven, P. Marmottant and M. Versluis, *Phys. Rev. Lett.*, 2008, **100**, 034504.
62 K. J. Humphry, A. Ajdari, A. Fernandez-Nieves, H. A. Stone and D. A. Weitz, *Phys. Rev. E: Stat., Nonlinear, Soft Matter Phys.*, 2009, **79**, 056310.
63 C. Priest, S. Herminghaus and R. Seemann, *Appl. Phys. Lett.*, 2006, **88**, 024106.
64 F. Malloggi, N. Pannacci, R. Attia, F. Monti, P. Mary, H. Willaime, P. Tabeling, B. Cabane and P. Poncet, *Langmuir*, 2010, **26**, 2369–2373.
65 S. Sugiura, M. Nakajima, S. Iwamoto and M. Seki, *Langmuir*, 2001, **17**, 5562–5566.
66 N. Bremond, A. R. Thiam and J. Bibette, *Phys. Rev. Lett.*, 2008, **100**, 024501.
67 L. Frenz, J. Blouwolff, A. D. Griffiths and J. C. Baret, *Langmuir*, 2008, **24**, 12073–12076.
68 B. Ahn, K. Lee, H. Lee, R. Panchapakesan and K. W. Oh, *Lab Chip*, 2011, **11**, 3956–3962.
69 A. M. Huebner, C. Abell, W. T. S. Huck, C. N. Baroud and F. Hollfelder, *Anal. Chem.*, 2011, **83**, 1462–1468.
70 P. Abbyad, R. Dangla, A. Alexandrou and C. N. Baroud, *Lab Chip*, 2011, **11**, 813–821.
71 L. G. Leal, *Phys. Fluids*, 2004, **16**, 1833–1851.
72 A. Yeung, T. Dabros, J. Masliyah and J. Czarnecki, *Colloids Surf., A*, 2000, **174**, 169–181.
73 L. Jorgensen, D. H. Kim, C. Vermehren, S. Bjerregaard and S. Frokjaer, *J. Pharm. Sci.*, 2004, **93**, 2994–3003.
74 R. M. Lorenz, J. S. Edgar, G. D. M. Jeffries and D. T. Chiu, *Anal. Chem.*, 2006, **78**, 6433–6439.
75 D. R. Link, S. L. Anna, D. A. Weitz and H. A. Stone, *Phys. Rev. Lett.*, 2004, **92**, 054503.
76 B. Zheng, J. D. Tice and R. F. Ismagilov, *Anal. Chem.*, 2004, **76**, 4977–4982.
77 L. H. Hung, K. M. Choi, W. Y. Tseng, Y. C. Tan, K. J. Shea and A. P. Lee, *Lab Chip*, 2006, **6**, 174–178.
78 T. Nisisako and T. Torii, *Lab Chip*, 2008, **8**, 287–293.

79 M. Hashimoto, S. S. Shevkoplyas, B. Zasonska, T. Szymborski, P. Garstecki and G. M. Whitesides, *Small*, 2008, **4**, 1795–1805.
80 V. Chokkalingam, S. Herminghaus and R. Seemann, *Appl. Phys. Lett.*, 2008, **93**, 254101.
81 V. Barbier, H. Willaime, P. Tabeling and F. Jousse, *Phys. Rev. E: Stat., Nonlinear, Soft Matter Phys.*, 2006, **74**, 046306.
82 R. Gupta, S. J. Baldock, P. Carreras, P. R. Fielden, N. J. Goddard, S. Mohr, B. S. Razavi and B. J. T. Brown, *Lab Chip*, 2011, **11**, 4052–4056.
83 F. Malloggi, S. A. Vanapalli, H. Gu, D. van den Ende and F. Mugele, *J. Phys.: Condens. Matter*, 2007, **19**, 462101.
84 H. Gu, C. U. Murade, M. H. G. Duits and F. Mugele, *Biomicrofluidics*, 2011, **5**, 011101.
85 Y. C. Tan, J. S. Fisher, A. I. Lee, V. Cristini and A. P. Lee, *Lab Chip*, 2004, **4**, 292–298.
86 W. H. Tan and S. Takeuchi, *Lab Chip*, 2006, **6**, 757–763.
87 X. Niu, S. Gulati, J. B. Edel and A. J. deMello, *Lab Chip*, 2008, **8**, 1837–1841.
88 K. Ahn, J. Agresti, H. Chong, M. Marquez and D. A. Weitz, *Appl. Phys. Lett.*, 2006, **88**, 264105.
89 J. Hong, M. Choi, J. B. Edel and A. J. deMello, *Lab Chip*, 2010, **10**, 2702–2709.
90 G. Cristobal, J. P. Benoit, M. Joanicot and A. Ajdari, *Appl. Phys. Lett.*, 2006, **89**, 034104.
91 A. R. Thiam, N. Bremond and J. Bibette, *Phys. Rev. Lett.*, 2011, **107**, 068301.
92 A. R. Thiam, N. Bremond and J. Bibette, *Langmuir*, 2012, **28**, 6291–6298.
93 D. Di Carlo, N. Aghdam and L. P. Lee, *Anal. Chem.*, 2006, **78**, 4925–4930.
94 Y. P. Bai, X. M. He, D. S. Liu, S. N. Patil, D. Bratton, A. Huebner, F. Hollfelder, C. Abell and W. T. S. Huck, *Lab Chip*, 2010, **10**, 1281–1285.
95 D. Langevin, *Adv. Colloid Interface Sci.*, 2000, **88**, 209–222.
96 D. Georgieva, V. Schmitt, F. Leal-Calderon and D. Langevin, *Langmuir*, 2009, **25**, 5565–5573.
97 R. Miller, P. Joos and V. B. Fainerman, *Adv. Colloid Interface Sci.*, 1994, **49**, 249–302.
98 R. Miller, R. Wustneck, J. Kragel and G. Kretzschmar, *Colloids Surf., A*, 1996, **111**, 75–118.
99 P. Erni, *Soft Matter*, 2011, **7**, 7586–7600.
100 F. Jin, R. Balasubramaniam and K. J. Stebe, *J. Adhes.*, 2004, **80**, 773–796.
101 J. H. Xu, S. W. Li, W. J. Lan and G. S. Luo, *Langmuir*, 2008, **24**, 11287–11292.
102 K. Wang, Y. C. Lu, J. H. Xu and G. S. Luo, *Langmuir*, 2009, **25**, 2153–2158.
103 M. L. J. Steegmans, A. Warmerdam, K. G. P. H. Schroen and R. M. Boom, *Langmuir*, 2009, **25**, 9751–9758.
104 J. D. Martin, J. N. Marhefka, K. B. Migler and S. D. Hudson, *Adv. Mater.*, 2011, **23**, 426–432.
105 S. D. Hudson, J. T. Cabral, W. J. Goodrum, K. L. Beers and E. J. Amis, *Appl. Phys. Lett.*, 2005, **87**, 081905.
106 G. I. Taylor, *Proc. R. Soc. London, Ser. A*, 1932, **138**, 41–48.
107 J. T. Cabral and S. D. Hudson, *Lab Chip*, 2006, **6**, 427–436.
108 J. D. Martin and S. D. Hudson, *New J. Phys.*, 2009, **11**, 115005.
109 A. Nadim and H. A. Stone, *Stud. Appl. Math.*, 1991, **85**, 53–73.
110 S. D. Hudson, *Rheol. Acta*, 2009, **49**, 237–243.
111 F. Mugele and J. C. Baret, *J. Phys.: Condens. Matter*, 2005, **17**, R705–R774.
112 A. G. Banpurkar, K. P. Nichols and F. Mugele, *Langmuir*, 2008, **24**, 10549–10551.
113 A. Ahmadi, K. D. Devlin, H. Najjaran, J. F. Holzman and M. Hoorfar, *Lab Chip*, 2010, **10**, 1429–1435.
114 A. G. Banpurkar, M. H. G. Duits, D. van den Ende and F. Mugele, *Langmuir*, 2009, **25**, 1245–1252.
115 B. Dai and L. G. Leal, *Phys. Fluids*, 2008, **20**, 040802.
116 D. Y. C. Chan, E. Klaseboer and R. Manica, *Adv. Colloid Interface Sci.*, 2011, **165**, 70–90.
117 A. Vrij, *Discuss. Faraday Soc.*, 1966, **42**, 23–33.
118 A. Sheludko, *Adv. Colloid Interface Sci.*, 1967, **1**, 391–464.
119 D. G. A. L. Aarts, M. Schmidt and H. N. W. Lekkerkerker, *Science*, 2004, **304**, 847–850.
120 A. J. de Vries, *Recl. Trav. Chim. Pays-Bas*, 2010, **77**, 383–399.
121 A. Kabalnov and H. Wennerstrom, *Langmuir*, 1996, **12**, 276–292.
122 L. Rekvig and D. Frenkel, *J. Chem. Phys.*, 2007, **127**, 134701.
123 D. Exerowa, D. Kashchiev and D. Platikanov, *Adv. Colloid Interface Sci.*, 1992, **40**, 201–256.
124 C. A. Helm, J. N. Israelachvili and P. M. McGuiggan, *Biochemistry*, 1992, **31**, 1794–1805.
125 P. G. de Gennes, *Chem. Eng. Sci.*, 2001, **56**, 5449–5450.
126 S. T. Thoroddsen, T. G. Etoh and K. Takehara, *Annu. Rev. Fluid Mech.*, 2008, **40**, 257–285.
127 N. Bremond, H. Domejean and J. Bibette, *Phys. Rev. Lett.*, 2011, **106**, 214502.
128 J. C. Baret, F. Kleinschmidt, A. El Harrak and A. D. Griffiths, *Langmuir*, 2009, **25**, 6088–6093.
129 A. S. Malcolm, A. F. Dexter, J. A. Katakdhond, S. I. Karakashev, A. V. Nguyen and A. P. J. Middelberg, *ChemPhysChem*, 2009, **10**, 778–781.
130 W. A. C. Bauer, J. Kotar, P. Cicuta, R. T. Woodward, J. V. M. Weaver and W. T. S. Huck, *Soft Matter*, 2011, **7**, 4214–4220.
131 C. Priest, M. D. Reid and C. P. Whitby, *J. Colloid Interface Sci.*, 2011, **363**, 301–306.
132 A. K. Chesters, *Chem. Eng. Res. Des.*, 1991, **69**, 259–270.
133 T. Krebs, K. Schroen and R. Boom, *Lab Chip*, 2012, **12**, 1060–1070.
134 C. N. Baroud, F. Gallaire and R. Dangla, *Lab Chip*, 2010, **10**, 2032–2045.
135 D. J. Chen, R. Cardinaels and P. Moldenaers, *Langmuir*, 2009, **25**, 12885–12893.
136 M. Loewenberg and E. J. Hinch, *J. Fluid Mech.*, 1997, **338**, 299–315.
137 S. Guido and M. Simeone, *J. Fluid Mech.*, 1998, **357**, 1–20.
138 Y. Yoon, M. Borrell, C. C. Park and L. G. Leal, *J. Fluid Mech.*, 2005, **525**, 355–379.
139 Y. Yoon, F. Baldessari, H. D. Ceniceros and L. G. Leal, *Phys. Fluids*, 2007, **19**, 102102.
140 A. Lai, N. Bremond and H. A. Stone, *J. Fluid Mech.*, 2009, **632**, 97–107.
141 D. Y. C. Chan, E. Klaseboer and R. Manica, *Soft Matter*, 2009, **5**, 2858–2861.
142 G. F. Christopher, J. Bergstein, N. B. End, M. Poon, C. Nguyen and S. L. Anna, *Lab Chip*, 2009, **9**, 1102–1109.
143 Y. L. Chen and J. Israelachvili, *Science*, 1991, **252**, 1157–1160.
144 R. Manica, J. Connor, L. Clasohm, S. Carnie, R. Horn and D. Chan, *Langmuir*, 2008, **24**, 1381–1390.
145 M. Zagnoni, C. N. Baroud and J. M. Cooper, *Phys. Rev. E: Stat., Nonlinear, Soft Matter Phys.*, 2009, **80**, 046303.
146 D. Z. Gunes, X. Clain, O. Breton, G. Mayor and A. S. Burbidge, *J. Colloid Interface Sci.*, 2010, **343**, 79–86.
147 B. Jose and T. Cubaud, *Microfluid. Nanofluid.*, 2011, **12**, 687–696.
148 J. Eggers, J. R. Lister and H. A. Stone, *J. Fluid Mech.*, 1999, **401**, 293–310.
149 J. S. Eow, M. Ghadiri, A. O. Sharif and T. J. Williams, *Chem. Eng. J.*, 2001, **84**, 173–192.
150 J. C. Baygents, N. J. Rivette and H. A. Stone, *J. Fluid Mech.*, 1998, **368**, 359–375.
151 G. I. Taylor, *Proc. R. Soc. London, Ser. A*, 1964, **280**, 383–397.
152 J. C. Weaver and Y. Chizmadzhev, *Bioelectrochem. Bioenerg.*, 1996, **41**, 135–160.
153 L. Landau and E. Lifchitz, *Physique théorique, tome 8: Electrodynamique des milieux continus*, Mir, 1990.
154 A. M. Ganan-Calvo, J. Davila and A. Barrero, *J. Aerosol Sci.*, 1997, **28**, 249–275.
155 D. Duft, T. Achtzehn, R. Muller, B. A. Huber and T. Leisner, *Nature*, 2003, **421**, 128.
156 R. T. Collins, J. J. Jones, M. T. Harris and O. A. Basaran, *Nat. Phys.*, 2007, **4**, 149–154.
157 M. H. Davis, *Q. J. Mech. Appl. Math.*, 1964, **17**, 499–511.
158 J. Latham and I. W. Roxburgh, *Proc. R. Soc. London, Ser. A*, 1966, **295**, 84–97.
159 G. I. Taylor, *Proc. R. Soc. London, Ser. A*, 1968, **306**, 423–434.
160 P. Atten, L. Lundgaard and G. Berg, *J. Electrost.*, 2006, **64**, 550–554.
161 G. I. Taylor, *Proc. R. Soc. London, Ser. A*, 1966, **291**, 159–166.
162 J. R. Melcher and G. I. Taylor, *Annu. Rev. Fluid Mech.*, 1969, **1**, 111–146.
163 D. A. Saville, *Annu. Rev. Fluid Mech.*, 1997, **29**, 27–64.
164 A. R. Thiam, N. Bremond and J. Bibette, *Phys. Rev. Lett.*, 2009, **102**, 188304.

165 A. C. Siegel, S. S. Shevkoplyas, D. B. Weibel, D. A. Bruzewicz, A. W. Martinez and G. M. Whitesides, *Angew. Chem., Int. Ed.*, 2006, **45**, 6877–6882.
166 J. C. Bird, W. D. Ristenpart, A. Belmonte and H. A. Stone, *Phys. Rev. Lett.*, 2009, **103**, 164502.
167 R. S. Allan and S. G. Mason, *J. Colloid Sci.*, 1962, **17**, 383–408.
168 W. D. Ristenpart, J. C. Bird, A. Belmonte, F. Dollar and H. A. Stone, *Nature*, 2009, **461**, 377–380.
169 N. Chetwani, S. Maheshwari and H.-C. Chang, *Phys. Rev. Lett.*, 2008, **101**, 204501.
170 M. M. Hohman, M. Shin, G. Rutledge and M. P. Brenner, *Phys. Fluids*, 2001, **13**, 2201–2220.
171 T. Szymborski, P. M. Korczyk, R. Holyst and P. Garstecki, *Appl. Phys. Lett.*, 2011, **99**, 094101.
172 C. Priest, S. Herminghaus and R. Seemann, *Appl. Phys. Lett.*, 2006, **89**, 134101.
173 X. Z. Niu, F. Gielen, A. J. deMello and J. B. Edel, *Anal. Chem.*, 2009, **81**, 7321–7325.
174 M. Zagnoni and J. M. Cooper, *Lab Chip*, 2009, **9**, 2652–2658.
175 M. Zagnoni, G. Le Lain and J. M. Cooper, *Langmuir*, 2010, **26**, 14443–14449.
176 P. Singh and N. Aubry, *Electrophoresis*, 2007, **28**, 644–657.
177 M. P. Aronson and H. M. Princen, *Nature*, 1980, **286**, 370–372.
178 P. Poulin and J. Bibette, *Phys. Rev. Lett.*, 1997, **79**, 3290–3293.
179 P. Poulin and J. Bibette, *Langmuir*, 1998, **14**, 6341–6343.
180 R. Lipowsky, *Nature*, 1991, **349**, 475–481.
181 V. M. Kaganer, H. Möhwald and P. Dutta, *Rev. Mod. Phys.*, 1999, **71**, 779–819.
182 F. Brochard-Wyart and P. G. de Gennes, *C. R. Phys.*, 2003, **4**, 281–287.
183 S. Pierrat, F. Brochard-Wyart and P. Nassoy, *Biophys. J.*, 2004, **87**, 2855–2869.
184 A. S. Smith, E. Sackmann and U. Seifert, *Phys. Rev. Lett.*, 2004, **92**, 208101.
185 P. Sens and H. Isambert, *Phys. Rev. Lett.*, 2002, **88**, 128102.
186 P. Claesson, T. Ederth, V. Bergeron and M. Rutland, *Adv. Colloid Interface Sci.*, 1996, **67**, 119–183.
187 O. Velev, G. Constantinides, D. Avraam, A. Payatakes and R. Borwankar, *J. Colloid Interface Sci.*, 1995, **175**, 68–76.
188 L. G. C. Pereira, C. Johansson, H. W. Blanch and C. J. Radke, *Colloids Surf., A*, 2001, **186**, 103–111.
189 F. Mostowfi, K. Khristov, J. Czarnecki, J. Masliyah and S. Bhattacharjee, *Appl. Phys. Lett.*, 2007, **90**, 184102.
190 F. Mostowfi, J. Czarnecki, J. Masliyah and S. Bhattacharjee, *J. Colloid Interface Sci.*, 2008, **317**, 593–603.
191 S. Thutupalli, S. Herminghaus and R. Seemann, *Soft Matter*, 2011, **7**, 1312–1320.
192 P. Taylor, *Adv. Colloid Interface Sci.*, 1998, **75**, 107–163.
193 B. Zheng, J. D. Tice, L. S. Roach and R. F. Ismagilov, *Angew. Chem., Int. Ed.*, 2004, **43**, 2508–2511.
194 H. N. Joensson, M. Uhlen and H. A. Svahn, *Lab Chip*, 2011, **11**, 1305–1310.
195 L. Boitard, D. Cottinet, C. Kleinschmitt, N. Bremond, J. Baudry, G. Yvert and J. Bibette, *Proc. Natl. Acad. Sci. U. S. A.*, 2012, **109**, 7181–7186.
196 M. Y. He, C. H. Sun and D. T. Chiu, *Anal. Chem.*, 2004, **76**, 1222–1227.
197 J. N. Lee, C. Park and G. M. Whitesides, *Anal. Chem.*, 2003, **75**, 6544–6554.
198 J. U. Shim, G. Cristobal, D. R. Link, T. Thorsen, Y. W. Jia, K. Piattelli and S. Fraden, *J. Am. Chem. Soc.*, 2007, **129**, 8825–8835.
199 J. Leng and J.-B. Salmon, *Lab Chip*, 2009, **9**, 24–34.
200 J. R. Burns and C. Ramshaw, *Lab Chip*, 2001, **1**, 10.
201 M. Kumemura and T. Korenaga, *Anal. Chim. Acta*, 2006, **558**, 75–79.
202 P. Mary, V. Studer and P. Tabeling, *Anal. Chem.*, 2008, **80**, 2680–2687.
203 W. Young, A. Pumir and Y. Pomeau, *Phys. Fluids A*, 1989, **1**, 462–469.
204 F. Courtois, L. F. Olguin, G. Whyte, A. B. Theberge, W. T. S. Huck, F. Hollfelder and C. Abell, *Anal. Chem.*, 2009, **81**, 3008–3016.
205 B. J. Zwolinski, H. Eyring and C. E. Reese, *J. Phys. Chem.*, 1949, **53**, 1426–1453.
206 M. B. Lande, J. M. Donovan and M. L. Zeidel, *J. Gen. Physiol.*, 1995, **106**, 67–84.
207 R. Dimova, N. Bezlyepkina, M. D. Jordo, R. L. Knorr, K. A. Riske, M. Staykova, P. M. Vlahovska, T. Yamamoto, P. Yang and R. Lipowsky, *Soft Matter*, 2009, **5**, 3201–3212.
208 Z. Vasilkoski, A. T. Esser, T. R. Gowrishankar and J. C. Weaver, *Phys. Rev. E: Stat., Nonlinear, Soft Matter Phys.*, 2006, **74**, 021904.
209 M. Zagnoni, *Lab Chip*, 2012, **12**, 1026–1039.
210 K. Funakoshi, H. Suzuki and S. Takeuchi, *Anal. Chem.*, 2006, **78**, 8169–8174.
211 H. Bayley, B. Cronin, A. Heron, M. A. Holden, W. L. Hwang, R. Syeda, J. Thompson and M. Wallace, *Mol. BioSyst.*, 2008, **4**, 1191–1208.